Matrices and X-ray tomography

Samuli Siltanen

Department of Mathematics and Statistics
University of Helsinki, Finland
samuli.siltanen@helsinki.fi
http://www.siltanen-research.net

Course: Applications of Matrix Computations
September 7, 2016

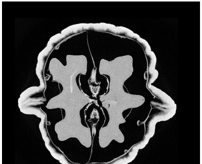 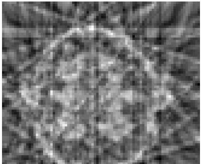 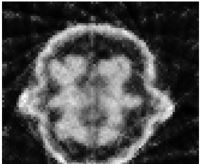 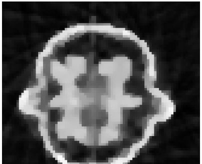

Finnish Centre of Excellence in Inverse Problems Research

ACADEMY OF FINLAND

OULUN YLIOPISTO UNIVERSITY of OULU

UNIVERSITY OF EASTERN FINLAND

UNIVERSITY OF JYVÄSKYLÄ

LAPPEENRANTA UNIVERSITY OF TECHNOLOGY

TAMPERE UNIVERSITY OF TECHNOLOGY

UNIVERSITY OF HELSINKI

http://wiki.helsinki.fi/display/inverse/Home

This my industrial-academic background

2009: Professor, University of Helsinki, Finland

2006: Professor, Tampere University of Technology, Finland

2005: R&D scientist at Palodex Group

2004: R&D scientist at GE Healthcare

2002: Postdoc at Gunma University, Japan

2000: R&D scientist at Instrumentarium Imaging

1999: PhD, Helsinki University of Technology, Finland

Outline

Wilhelm Conrad Röntgen invented X-rays and was awarded the first Nobel Prize in Physics in 1901

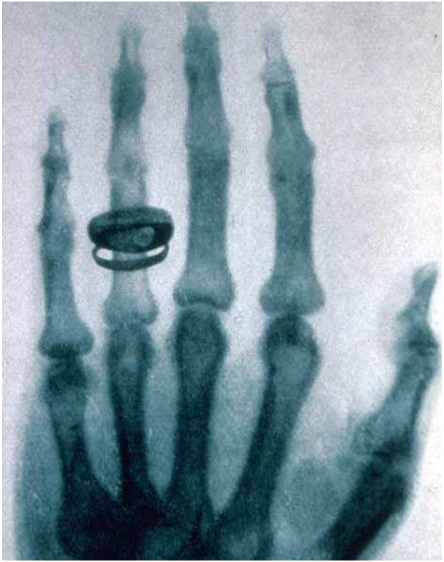

Godfrey Hounsfield and Allan McLeod Cormack were the first to develop X-ray tomography

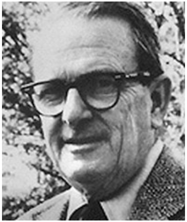

Hounsfield (top) and Cormack received Nobel prizes in 1979.

Godfrey Hounsfield and Allan McLeod Cormack were the first to develop X-ray tomography

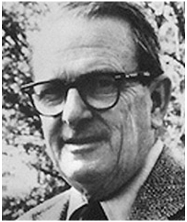

Hounsfield (top) and Cormack received Nobel prizes in 1979.

Godfrey Hounsfield and Allan McLeod Cormack were the first to develop X-ray tomography

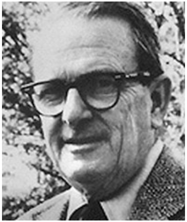

Hounsfield (top) and Cormack received Nobel prizes in 1979.

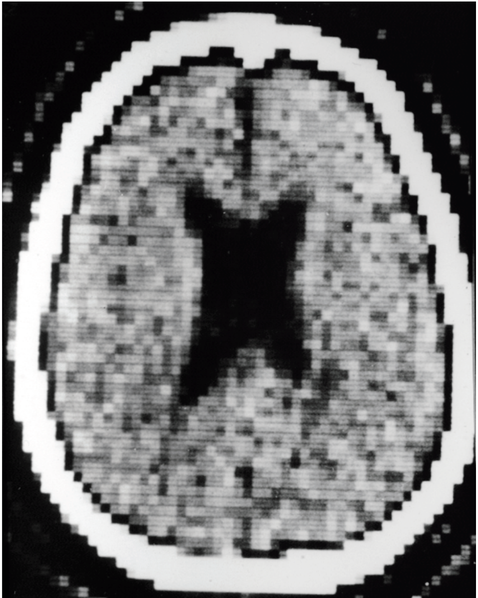

Reconstruction of a function from its line integrals was first invented by Johann Radon in 1917

Johann Radon (1887-1956)

$$f(P) = -\frac{1}{\pi}\int_0^\infty \frac{d\overline{F_p}(q)}{q}$$

Traditional X-ray tomography requires many projection images using small angular steps

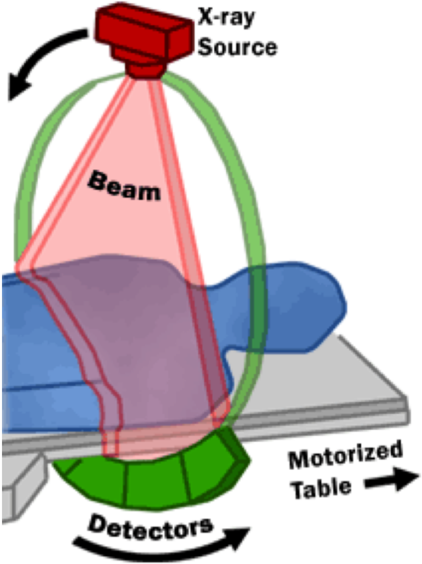

$$\frac{1}{4\pi^2}\int_{S^1}\int_{\mathbb{R}} \frac{\frac{d}{ds}(Rf)(\theta, s)}{x\cdot\theta - s}\,ds\,d\theta$$

Contrast-enhanced CT of abdomen, showing liver metastases

Head CT can be used for detecting and monitoring brain hemorrhage

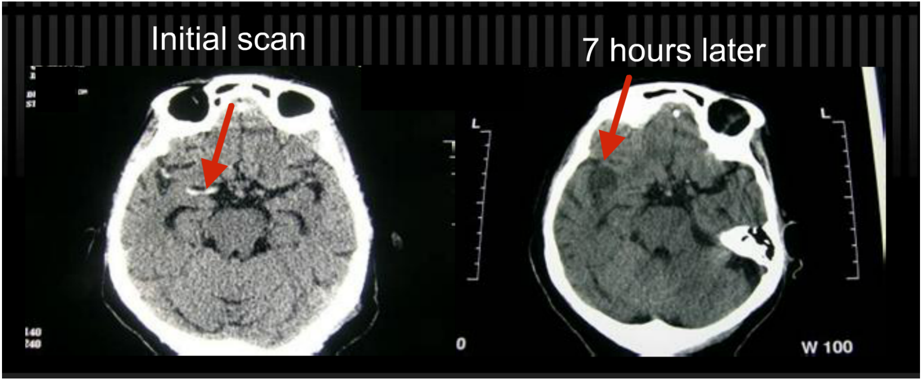

Source: LearningRadiology.com

Unusual variant of the Nutcracker Fracture of the calcaneus and tarsal navicular

Axial slice of the right foot

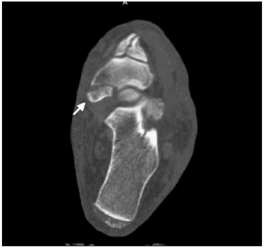

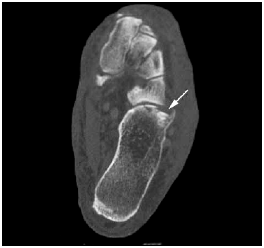

Another axial slice

Sagittal slice

3D render

[Gajendran, Yoo & Hunter, Radiology Case Reports **3** (2008)]

Outline

X-ray intensity attenuates inside matter, here shown with a homogeneous block

https://www.youtube.com/watch?v=IfXo2S1xXCQ

X-ray intensity attenuates inside matter, here shown with two homogeneous blocks

https://www.youtube.com/watch?v=Z_IBFQcn0l8

We can consider a more complicated case, here the Shepp-Logan phantom

https://www.youtube.com/watch?v=5T1oBfBL1Tg

A digital X-ray detector counts how many photons arrive at each pixel

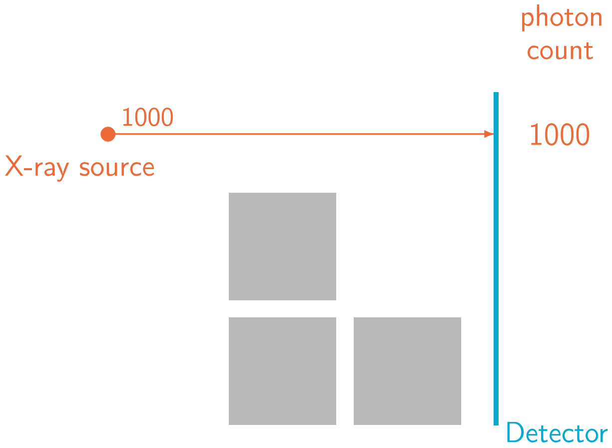

Adding material between the source and detector reveals the exponential X-ray attenuation law

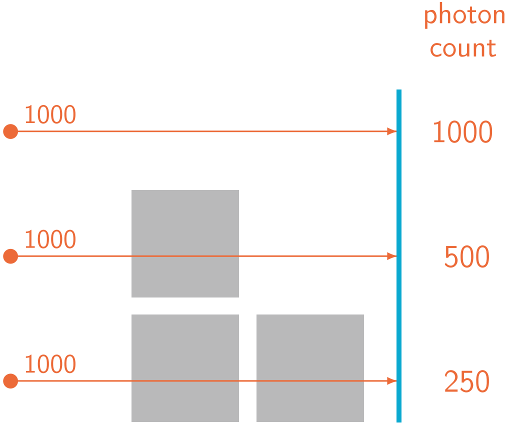

We take logarithm of the photon counts to compensate for the exponential attenuation law

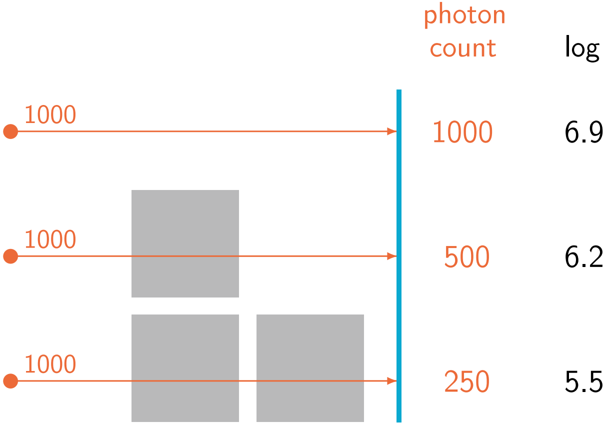

Final calibration step is to subtract the logarithms from the empty space value (here 6.9)

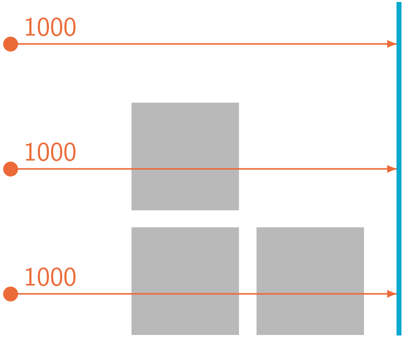

photon count	log	line integral
1000	6.9	**0.0**
500	6.2	**0.7**
250	5.5	**1.4**

After calibration we are observing how much attenuating matter the X-ray encounters

https://www.youtube.com/watch?v=5LK-p0U1sl0

We can consider a more complicated case, here the Shepp-Logan phantom

https://www.youtube.com/watch?v=TKqcrDGPsAI

This sweeping movement is the data collection mode of first-generation CT scanners

https://www.youtube.com/watch?v=TbLaQo3rgEE

Rotating around the object allows us to form the so-called *sinogram*

https://www.youtube.com/watch?v=5Vyc1TzmNI8

This is an illustration of the standard reconstruction by filtered back-projection

https://www.youtube.com/watch?v=ddZeLNh9aac

Outline

We write the reconstruction problem in matrix form

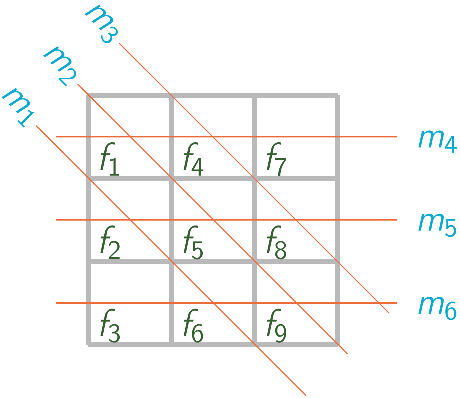

$$f = \begin{bmatrix} f_1 \\ f_2 \\ f_3 \\ f_4 \\ f_5 \\ f_6 \\ f_7 \\ f_8 \\ f_9 \end{bmatrix}, \quad m = \begin{bmatrix} m_1 \\ m_2 \\ m_3 \\ m_4 \\ m_5 \\ m_6 \end{bmatrix},$$

Measurement model: $m = Af + \varepsilon$

This is the matrix equation related to the above measurement

$$
\begin{bmatrix} m_1 \\ m_2 \\ m_3 \\ m_4 \\ m_5 \\ m_6 \end{bmatrix} =
\begin{bmatrix}
0 & \sqrt{2} & 0 & 0 & 0 & \sqrt{2} & 0 & 0 & 0 \\
\sqrt{2} & 0 & 0 & 0 & \sqrt{2} & 0 & 0 & 0 & \sqrt{2} \\
0 & 0 & 0 & \sqrt{2} & 0 & 0 & 0 & \sqrt{2} & 0 \\
1 & 0 & 0 & 1 & 0 & 0 & 1 & 0 & 0 \\
0 & 1 & 0 & 0 & 1 & 0 & 0 & 1 & 0 \\
0 & 0 & 1 & 0 & 0 & 1 & 0 & 0 & 1
\end{bmatrix}
\begin{bmatrix} f_1 \\ f_2 \\ f_3 \\ f_4 \\ f_5 \\ f_6 \\ f_7 \\ f_8 \\ f_9 \end{bmatrix} +
\begin{bmatrix} \varepsilon_1 \\ \varepsilon_2 \\ \varepsilon_3 \\ \varepsilon_4 \\ \varepsilon_5 \\ \varepsilon_6 \end{bmatrix}
$$

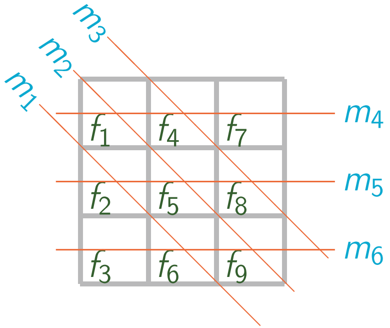

This is the matrix equation related to the above measurement

$$
\begin{bmatrix} m_1 \\ m_2 \\ m_3 \\ m_4 \\ m_5 \\ m_6 \end{bmatrix}
=
\begin{bmatrix}
0 & \sqrt{2} & 0 & 0 & 0 & \sqrt{2} & 0 & 0 & 0 \\
\sqrt{2} & 0 & 0 & 0 & \sqrt{2} & 0 & 0 & 0 & \sqrt{2} \\
0 & 0 & 0 & \sqrt{2} & 0 & 0 & 0 & \sqrt{2} & 0 \\
1 & 0 & 0 & 1 & 0 & 0 & 1 & 0 & 0 \\
0 & 1 & 0 & 0 & 1 & 0 & 0 & 1 & 0 \\
0 & 0 & 1 & 0 & 0 & 1 & 0 & 0 & 1
\end{bmatrix}
\begin{bmatrix} f_1 \\ f_2 \\ f_3 \\ f_4 \\ f_5 \\ f_6 \\ f_7 \\ f_8 \\ f_9 \end{bmatrix}
+
\begin{bmatrix} \varepsilon_1 \\ \varepsilon_2 \\ \varepsilon_3 \\ \varepsilon_4 \\ \varepsilon_5 \\ \varepsilon_6 \end{bmatrix}
$$

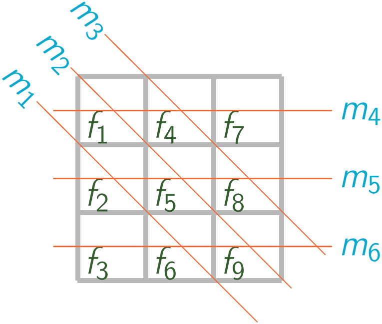

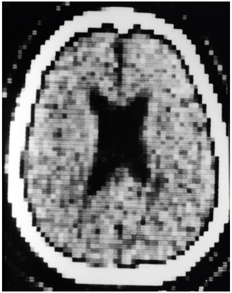

Original image by G. Hounsfield from the 1970's

This is Professor Keijo Hämäläinen’s X-ray lab

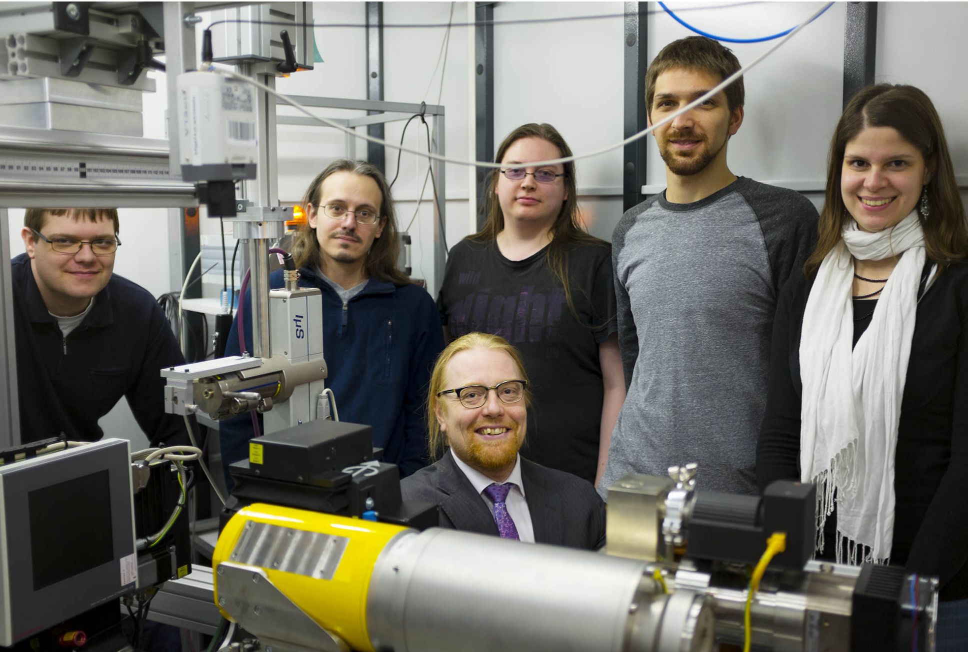

We collected X-ray projection data of a walnut from 1200 directions

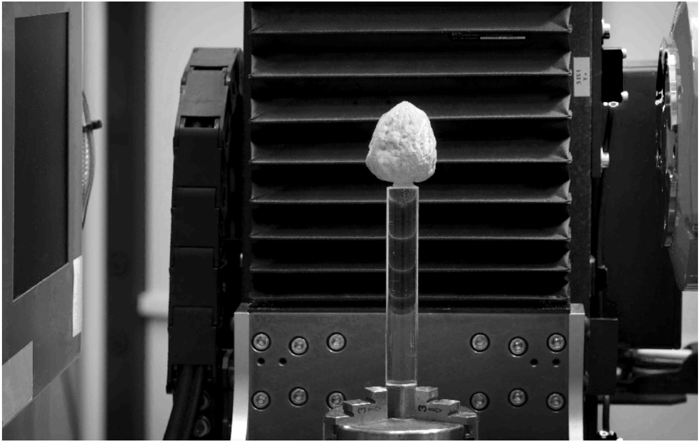

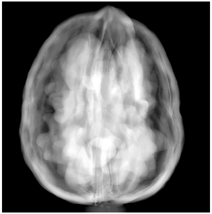

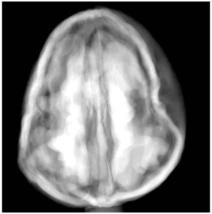

Laboratory and data collection by Keijo Hämäläinen and Aki Kallonen, University of Helsinki.

The data is openly available at http://fips.fi/dataset.php, thanks to Esa Niemi and Antti Kujanpää

Reconstructions of a 2D slice through the walnut using filtered back-projection (FBP)

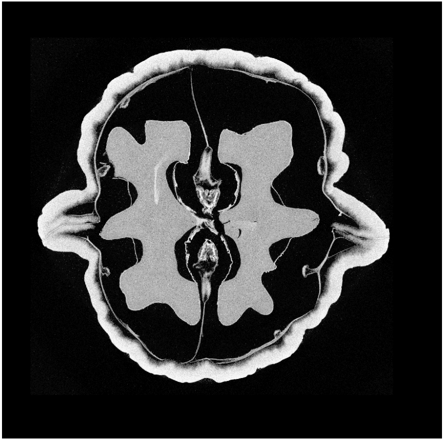

FBP with comprehensive data
(1200 projections)

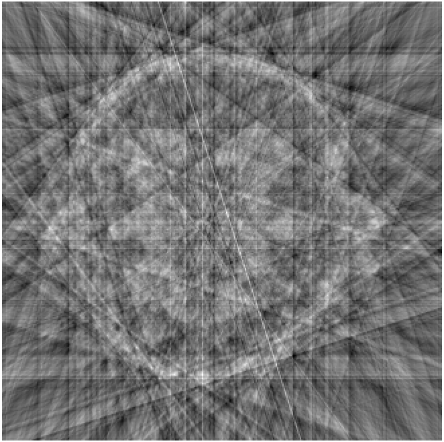

FBP with sparse data
(20 projections)

Sparse-data reconstruction of the walnut using non-negative Landweber iteration

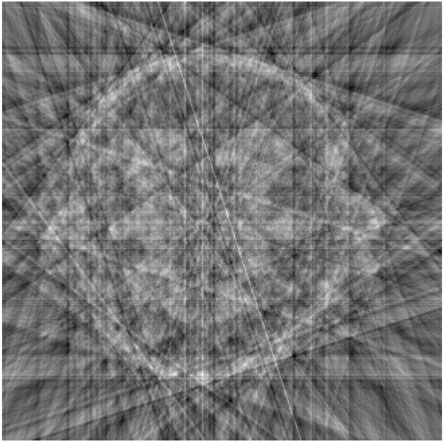

Filtered back-projection

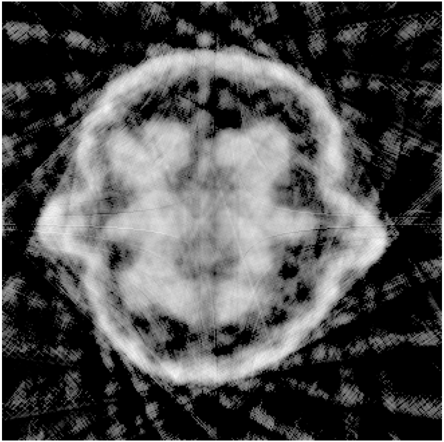

Sparse-data reconstruction of the walnut using non-negative total variation regularization

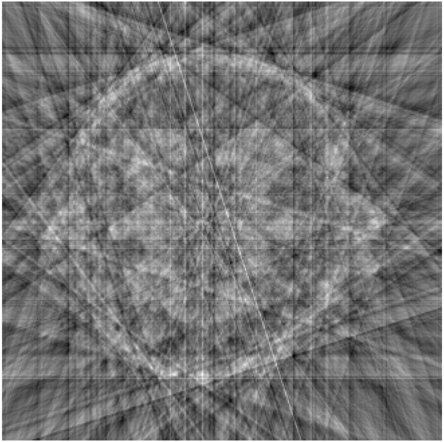

Filtered back-projection

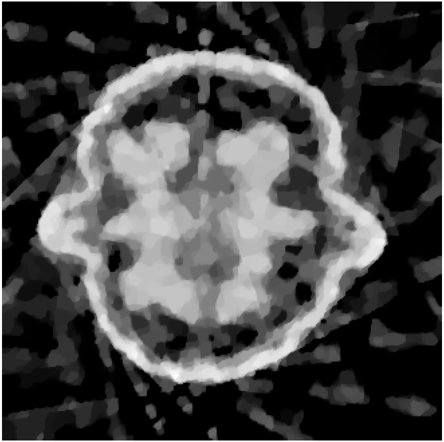

Constrained TV regularization

$$\arg\min_{f\in\mathbb{R}^n_+} \left\{ \|Af - m\|_2^2 + \alpha \|\nabla f\|_1 \right\}$$

Sparse-data reconstruction of the walnut using Haar wavelet sparsity

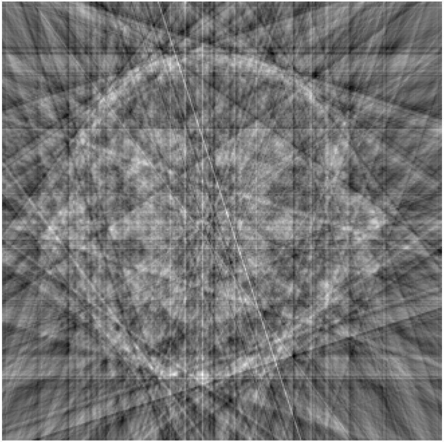

Filtered back-projection

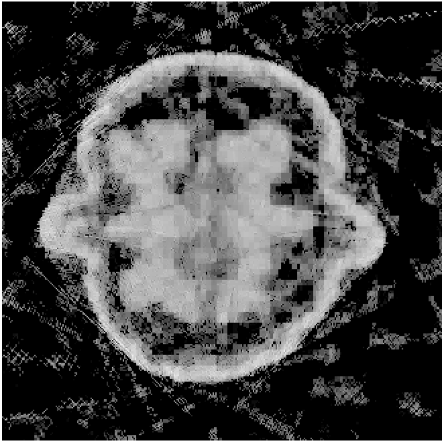

Constrained Besov regularization

$$\arg\min_{f \in \mathbb{R}^n_+} \left\{ \|Af - m\|_2^2 + \alpha \|f\|_{B^1_{11}} \right\}$$

Outline

Background

Principle of X-ray tomography

Total variation regularized tomography

Industrial case study: low-dose dental imaging

Another application: ozone layer monitoring

The VT device was developed in 2001–2012 by

Lauri Harhanen
Nuutti Hyvönen
Seppo Järvenpää
Jari Kaipio
Martti Kalke
Petri Koistinen
Ville Kolehmainen
Matti Lassas
Jan Moberg
Kati Niinimäki
Juha Pirttilä
Maaria Rantala
Eero Saksman
Henri Setälä
Erkki Somersalo
Antti Vanne
Simopekka Vänskä
Richard L. Webber

INSTRUMENTARIUM imaging

GE Healthcare

PALODEX GROUP

Tekes

Application: dental implant planning, where a missing tooth is replaced with an implant

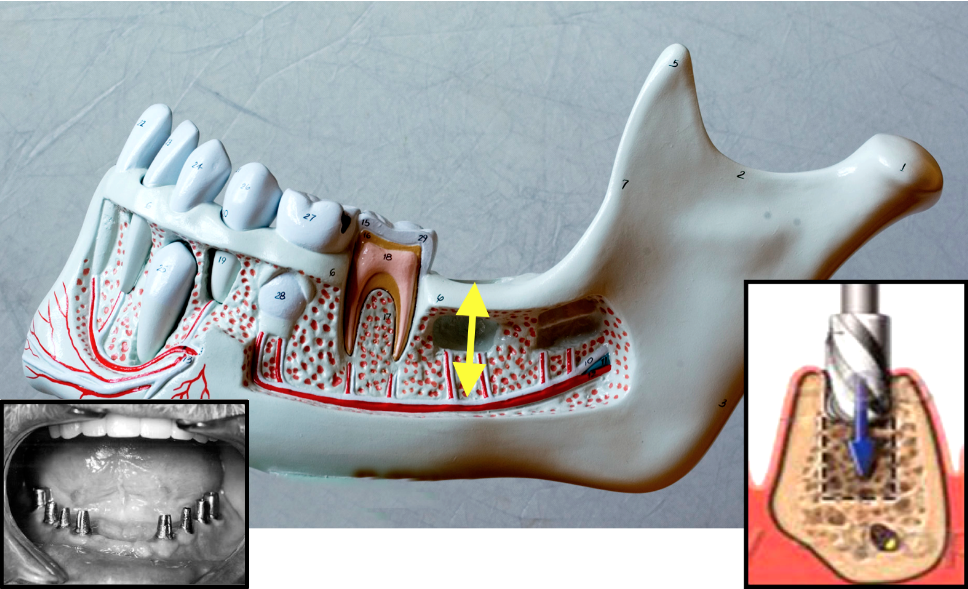

Nowadays, a digital panoramic imaging device is standard equipment at dental clinics

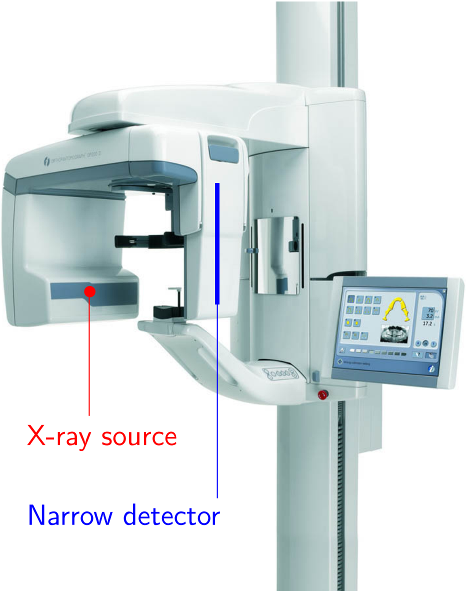

A panoramic dental image offers a general overview showing all teeth and other dento-maxillofacial structures simultaneously.

Panoramic images are not suitable for dental implant planning because of unavoidable geometric distortion.

Panoramic dental imaging shows all the teeth simultaneously

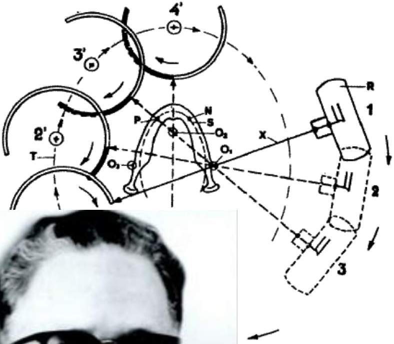

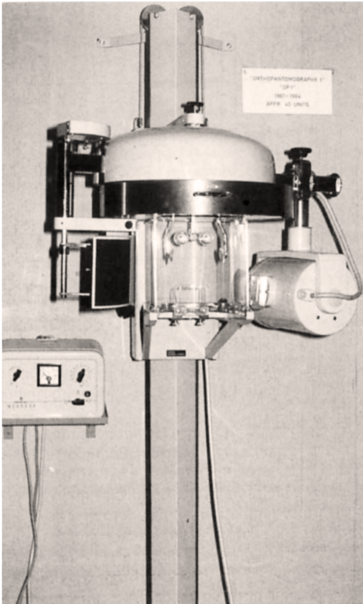

Panoramic imaging was invented by Yrjö Veli Paatero in the 1950's.

We reprogram the panoramic X-ray device so that it collects projection data by scanning

https://www.youtube.com/watch?v=motthjiP8ZQ

We reprogram the panoramic X-ray device so that it collects projection data by scanning

Number of projection images: **11**

Angle of view: **40 degrees**

Image size: **1000×1000 pixels**

The unknown vector f has **7 000 000** elements.

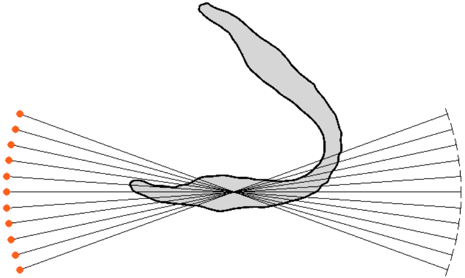

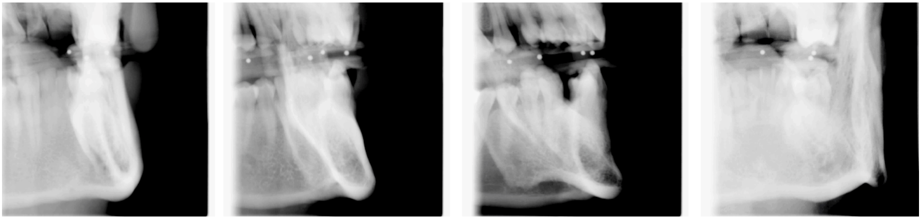

Here are example images of an actual patient: navigation image (left) and desired slice (right).

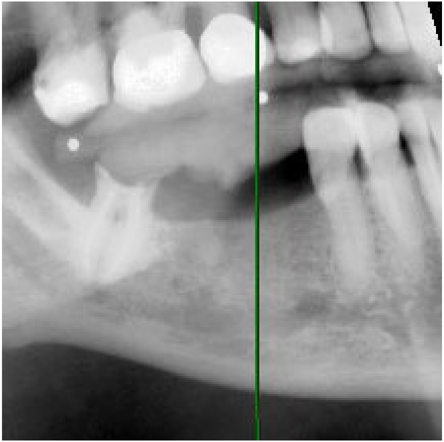

Kolehmainen, Vanne, S, Järvenpää, Kaipio, Lassas & Kalke **2006**, Kolehmainen, Lassas & S **2008**

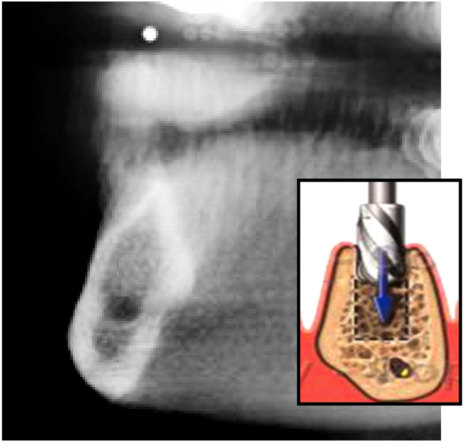

Cederlund, Kalke & Welander **2009**, Hyvönen, Kalke, Lassas, Setälä & S **2010**, U.S. patent 7269241

The radiation dose of the VT device is lowest among 3D dental imaging modalities

Modality	μSv
Head CT	2100
CB Mercuray	558
i-Cat	193
NewTom 3G	59
VT device	**13**

[Ludlow, Davies-Ludlow, Brooks & Howerton **2006**]

The VT device has been available in the international market since 2008.

Here the CBCT reconstruction (right) gave 100 times more radiation than VT imaging (middle)

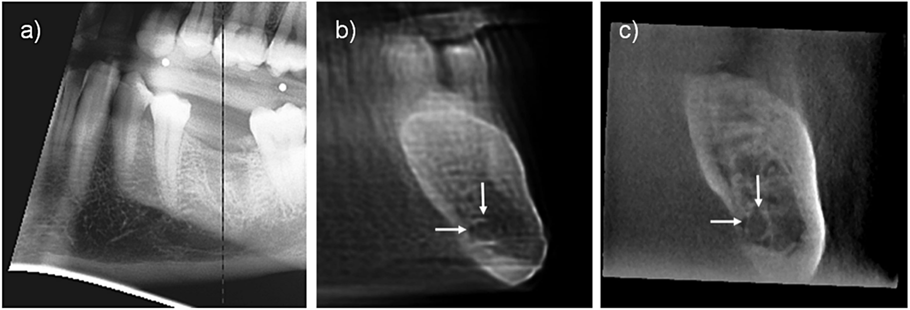

Images from the PhD thesis of Martti Kalke.

This is my new X-ray laboratory at University of Helsinki

Outline

The mathematics of X-ray tomography can be used for recovering the ozone layer

European Space Agency
Finnish Meteorological Institute
Envisat and GOMOS projects